

The Dynamics of Unsteady Detonation with Diffusion

Christopher M. Romick *

Department of Aerospace and Mechanical Engineering, University of Notre Dame, Notre Dame, Indiana 46556

Tariq D. Aslam †

Dynamic and Energetic Materials Division, Los Alamos National Laboratory, Los Alamos, New Mexico 87545

Joseph M. Powers ‡

Department of Aerospace and Mechanical Engineering, University of Notre Dame, Notre Dame, Indiana 46556

The dynamics of one-dimensional detonations predicted by a one-step irreversible Arrhenius kinetic model with the inclusion of mass, momentum, and energy diffusion were investigated. A series of calculations in which activation energy is varied, holding the length scales of diffusion and reaction constant, was performed. As in the inviscid case, as the activation energy increases, the system goes through a period-doubling process and eventually undergoes a transition to chaos. Within the chaotic regime, there exist regions of low frequency limit cycles. An approximation to Feigenbaum's constant, the rate at which bifurcation points converge, is obtained. The addition of diffusion significantly delays the onset of instability and strongly influences the dynamics in the unstable regime. Because the selected reaction and viscous length scales are representative of real physical systems, the common use of reactive Euler equations to predict detonation dynamics in the unstable and marginally stable regimes is called into question; reactive Navier-Stokes may be a more appropriate model in such regimes.

I. Introduction

It is a common notion in detonation theory that the effects of diffusion can be neglected in comparison to those of reaction and advection, *cf.* Fedkiw *et al.*,¹ Oran *et al.*,² Hu *et al.*,³ Wang *et al.*,⁴ Walter and da Silva,⁵ He and Karagozian,⁶ Aslam and Powers,⁷ or Tsuboi *et al.*⁸ However, there are indications that such an assumption can be problematic. For example, using grid sizes around 10^{-6} m for their three-dimensional simulations of unsteady H_2 -air detonations, Tsuboi *et al.* report wave dynamics that show strong sensitivity to the fineness of the grid. While apparent convergence of some structures was reported, they also note with regard to some particulars of the detonation structure "The present results cannot resolve such cross-hatchings in the ribbon because of a lack of grid resolution." The presence of reaction dynamics and steep gradients at micron length scales suggests that in fact physical diffusion has an important role to play. Indeed, Powers⁹ showed that two-dimensional detonation patterns are strongly grid-dependent for simulations of reactive Euler equations, but relax to a grid-independent dissipative structure for a comparable reactive Navier-Stokes calculation. This suggests numerical diffusion is actually playing a significant role in the inviscid calculations and that one should consider the introduction of grid-independent physical diffusion to properly capture the dynamics.

Consideration of the reaction-advection length scales admitted by an inviscid detonation explains why such fine scales are necessary. Powers and Paolucci¹⁰ performed a spatial eigenvalue analysis on a detailed kinetic H_2 -air model and showed for inviscid detonations that the length scales for a steady Chapman-Jouguet (CJ) detonation can span five orders of magnitude near equilibrium, with the smallest length scale for an ambient mixture at atmospheric pressure being 10^{-7} m and the largest being 10^{-2} m; away from

*Ph.D. Candidate, AIAA Member, romick@nd.edu.

†Technical Staff Member, AIAA Member, aslam@lanl.gov.

‡Professor, AIAA Associate Fellow, powers@nd.edu.

© C. M. Romick, 2011

equilibrium the breadth of scales can be even larger. These fine reaction scales are a manifestation of an averaged representation of the molecular collision model in which the fundamental length scale is the mean free path.¹¹ In order to have a mathematically verified prediction, this wide range of scales must be resolved, which poses a daunting task.

The choice of a one-step kinetic model induces a single reaction scale, in contrast to the multiple reaction scales of detailed kinetic models. This allows for the effects of the interplay between chemistry and transport phenomena on detonations be more easily studied. Such a model has been studied extensively; the stability and non-linear dynamics are well understood in the inviscid limit, *cf.* Erpenbeck,¹² Lee and Stewart,¹³ Bourlioux *et al.*,¹⁴ Sharpe,¹⁵ Kasimov and Stewart,¹⁶ Ng *et al.*,¹⁷ or Henrick *et al.*¹⁸ Erpenbeck started investigation into linear stability of detonations nearly fifty years ago. Lee and Stewart developed a normal-mode approach to the linear stability of the idealized detonation to one-dimensional perturbations using a shooting method to find the unstable modes. Bourlioux *et al.* study the nonlinear development of instability. Kasimov and Stewart also applied a normal mode approach to the linear stability problem and performed a numerical analysis using a first order shock-fitting technique. Ng *et al.* developed a coarse bifurcation diagram showing how the oscillatory behavior became progressively more complex as activation energy increased. Henrick *et al.* developed a more detailed bifurcation diagram using a true fifth order shock-fitting method in combination with a mapped WENO scheme. In two dimensions, Watt and Sharpe¹⁹ used a one-step inviscid model and concluded “resolved and accurate calculations of the cellular dynamics are currently computationally prohibitive, even with a dynamically adaptive numerical scheme.”

The goal of this paper is to predict the effects of diffusion on the long-time dynamics of a detonation described by one-step kinetics. The plan of the paper is as follows. First the mathematical model is presented. This is followed by a description of the computational method. The model is used to predict the viscous analog of the period-doubling phenomena predicted in the inviscid limit by Sharpe, Ng *et al.*, and Henrick *et al.* The convergence of the period-doubling bifurcation points is shown to be in agreement with the general theory of Feigenbaum,^{20,21} and diffusion is seen to have a generally stabilizing effect on detonation dynamics.

II. Mathematical Model

The model equations adopted here are the one-dimensional unsteady compressible reactive Navier-Stokes equations with one-step kinetics:

$$\frac{\partial \rho}{\partial t} + \frac{\partial}{\partial x} (\rho u) = 0, \quad (1)$$

$$\frac{\partial}{\partial t} (\rho u) + \frac{\partial}{\partial x} (\rho u^2 + P - \tau) = 0, \quad (2)$$

$$\frac{\partial}{\partial t} \left(\rho \left(e + \frac{u^2}{2} \right) \right) + \frac{\partial}{\partial x} \left(\rho u \left(e + \frac{u^2}{2} \right) + j^q + (P - \tau) u \right) = 0, \quad (3)$$

$$\frac{\partial}{\partial t} (\rho \lambda) + \frac{\partial}{\partial x} (\rho u \lambda + j_\lambda^m) = \rho r, \quad (4)$$

where the independent variables are time, t , and the spatial coordinate, x . In Eqs. (1-4), ρ is the mass density, u the particle velocity, P the pressure, τ the diffusive viscous stress, e the specific internal energy, j^q the diffusive heat flux, λ the reaction progress variable, j_λ^m the diffusive mass flux, and r the reaction rate. The equations were transformed to a frame of reference moving at a constant velocity, D . Applying this Galilean transformation, one recovers

$$\frac{\partial \rho}{\partial t} + \frac{\partial}{\partial x} (\rho (u - D)) = 0, \quad (5)$$

$$\frac{\partial}{\partial t} (\rho u) + \frac{\partial}{\partial x} (\rho u (u - D) + P - \tau) = 0, \quad (6)$$

$$\frac{\partial}{\partial t} \left(\rho \left(e + \frac{u^2}{2} \right) \right) + \frac{\partial}{\partial x} \left(\rho (u - D) \left(e + \frac{u^2}{2} \right) + j^q + (P - \tau) u \right) = 0, \quad (7)$$

$$\frac{\partial}{\partial t} (\rho \lambda) + \frac{\partial}{\partial x} (\rho (u - D) \lambda + j_\lambda^m) = \rho r. \quad (8)$$

The particle velocity, u , is still measured in the laboratory frame in Eqs. (5-8). The constitutive relations chosen for mass, momentum, and energy diffusion are

$$j_\lambda^m = -\rho \mathcal{D} \frac{\partial \lambda}{\partial x}, \quad (9)$$

$$\tau = \frac{4}{3} \mu \frac{\partial u}{\partial x}, \quad (10)$$

$$j^q = -k \frac{\partial T}{\partial x} + \rho \mathcal{D} q \frac{\partial \lambda}{\partial x}, \quad (11)$$

where Fick's Law for binary diffusion has been adopted as the model for diffusive mass flux, \mathcal{D} is the mass diffusion coefficient, μ the dynamic viscosity, k the thermal conductivity, T the temperature, and q the heat release. A calorically perfect ideal gas model is adopted:

$$P = \rho R T, \quad (12a)$$

$$e = \frac{P}{\rho(\gamma - 1)} - q\lambda, \quad (12b)$$

where R is the gas constant, and γ is the ratio of specific heats. The simple irreversible one-step reaction model was chosen to be $A \rightarrow B$, where A and B are the reactant and product, respectively; both have identical molecular masses and specific heats. In the undisturbed state, only A is present. The mass fractions of A and B are given by $1 - \lambda$, and λ , respectively. The reaction rate r is taken to be given by the law of mass action with an Arrhenius rate sensitivity:

$$r = H(P - P_s) a (1 - \lambda) e^{-\frac{\tilde{E}}{P/\rho}}. \quad (13)$$

Here a is the collision frequency factor, \tilde{E} the activation energy, and $H(P - P_s)$ is a Heaviside function which suppresses reaction when $P < P_s$, where P_s is a selected pressure. Also note the ambient pressure and density are taken to be P_o and ρ_o , respectively.

III. Computational Method and Verification

A temporally explicit point-wise method of lines approach is used. This method allows separate temporal and spatial discretizations and also allows for the inclusion of source terms. The advective terms were calculated using a combination of a fifth order WENO scheme and Lax-Friedrichs discretization;²² the diffusive terms are treated with sixth order central differences. As an aside, it is noted that a fifth order central differencing of the advection terms would work as well as a fifth order WENO discretization because the solutions contain no discontinuities. Temporal integration is accomplished using a third order Runge-Kutta scheme.

The exercise of demonstrating the harmony of the discrete solution with the foundational mathematics is known as verification.²³ The method of manufactured solutions²⁴ was used to verify the code. In this method, a solution form is assumed, and special source terms are added to the governing equations in such a fashion that the assumed solution satisfies the modified equations. A periodic form for the solution was assumed

$$\rho(x, t) = a_1 + b_1 \cos[\pi(x - t)], \quad (14)$$

$$u(x, t) = a_2 + b_2 \cos[\pi(x - t)], \quad (15)$$

$$p(x, t) = a_3 + b_3 \cos[\pi(x + t)], \quad (16)$$

$$\lambda(x, t) = a_4 + b_4 \cos[\pi(x + t)], \quad (17)$$

with a domain $x \in [-1, 1]$. The coefficients are taken to be $a_1 = a_2 = a_3 = a_4 = 1$ and $b_2 = b_3 = b_4 = 1/10, b_1 = 1$. The initial conditions are those given by Eqs. (14-17) at $t = 0$. The source terms that this exact solution generates are straightforwardly found by direct substitution into the governing equations. However, they are lengthy and not presented here. Figure 1 shows fifth order asymptotic convergence of the error of the discrete approximation as the spatial grid is refined. The ordinate is the sum of all variables' L_1 errors normalized by the maximum value of the variable. It is noted that for convergence of the reactive Navier-Stokes equations, the presence of the Heaviside step function in the reaction rate term may preclude a full fifth order convergence rate.

IV. Results

Here simulations of the reactive Navier-Stokes equations are presented. All calculations were performed in a single processor environment on an AMD 2.4 GHz processor with 512 kB cache. The simulation is initialized with the inviscid Zel'dovich-von Neumann-Döring (ZND) solution in a moving frame traveling at the CJ speed. Each simulation is integrated in time to determine the long time behavior. For a calculation of $2.5 \mu s$ the computational time required was two days. Some calculations took as long as nine days for full relaxation.

By selecting the diffusion coefficient, $\mathcal{D} = 10^{-4} m^2/s$, thermal conductivity, $k = 10^{-1} W/m/K$, and viscosity, $\mu = 10^{-4} Ns/m^2$ the Lewis, Le , Prandtl, Pr , and Schmidt, Sc numbers evaluated at the ambient density, $\rho_o = 1 kg/m^3$, are unity. All of these parameters are within an order of magnitude of gases at a slightly elevated temperature. In the inviscid detonation, the activation energy controls the stability of the system; the rate constant merely introduces a length scale, the half reaction length, $L_{1/2}$, (the distance between the inviscid shock and the location at which $\lambda = 1/2$). If $L_{1/2}$ is fixed, the effect of diffusion on the system can be explored. Using simple dimensional analysis of advection and diffusion parameters ($U = 1000 m/s$ was chosen as a typical velocity scale) gives rise to an approximate length scale of mass diffusion, $\mathcal{D}/U = 10^{-7} m$, and likewise for momentum and energy diffusion $\mu/\rho_o/U = 10^{-7} m$, and $k/\rho_o/C_p/U = 10^{-7} m$. Since all the diffusion length scales are the same, let that scale be denoted as $L_\mu = 10^{-7} m$. The chosen parameters in the governing equations are $P_o = 101325 Pa$, $P_s = 200000 Pa$, $\rho_o = 1 kg/m^3$, $q = 5066250 m^2/s^2$, $\gamma = 6/5$, and $\tilde{E} \in [2533125, 3232400] m^2/s^2$. With this heat release, D_{CJ} for the inviscid problem is

$$D_{CJ} = \sqrt{\gamma \frac{P_o}{\rho_o} + \frac{q(\gamma^2 - 1)}{2}} + \sqrt{\frac{q(\gamma^2 - 1)}{2}} = 2167.56 \frac{m}{s}. \quad (18)$$

To compare directly with previous work in the inviscid limit, the activation energies will be presented in dimensionless form, $E = \tilde{E} / (1.01325 \times 10^5 m^2/s^2)$, thus $E \in [25, 32]$. Using these parameters allows for the interaction of diffusion and reaction effects to be easily studied. Moreover, these parameters induce a set of scales which are of similar orders of magnitude to those given in reactive Navier-Stokes models with detailed chemical kinetics. Unless otherwise stated, the calculations presented are for a ratio of $L_\mu/L_{1/2} = 1/10$.

A. Effect of diffusion on limit cycle behavior

In the inviscid case, linear stability analysis by Lee and Stewart revealed that for $E < 25.26$, the steady ZND wave is linearly stable and is otherwise linearly unstable. The activation energy at this stability boundary is labeled E_0 . For the same case Henrick *et al.* numerically found the stability limit at $E_0 = 25.265 \pm 0.005$, which is in excellent agreement with the prediction of linear stability analysis. We examine a viscous case well above the inviscid stability limit, $E = 26.647$, which Henrick *et al.* found to relax to a period-1 limit cycle for an inviscid simulation. In our viscous simulation, it can be seen from Fig. 2 that there is no limit cycle behavior, and the detonation predicted by viscous theory is in fact a stable steadily propagating wave. The stability boundary for the viscous case is found at $E_0 \approx 27.1404$. A period-1 limit cycle may be realized in the viscous case by increasing the activation energy above E_0 ; we show an example for $E = 27.6339$ in Fig. 3.

B. Effect of diffusion on transition to chaos

For higher values of E , more complicated dynamics are predicted. A period-doubling behavior and transition to chaos for unstable detonations were found to be remarkably similar to that predicted by the simple logistic map.^{25,26} The activation energy at which the behavior switches from a period- 2^{n-1} to a period- 2^n solution is denoted as E_n , for $n \geq 1$. As predicted by Sharpe and Ng *et al.* and shown in Henrick *et al.*, transition to a period-2 oscillation occurs at $E_1 \approx 27.2$ in the inviscid case. For the viscous case, we find instead $E_1 \approx 29.3116$; Fig. 4(a) shows the time history of the detonation pressure for a slightly higher $E = 29.6077$, which shows in the long time limit two distinct relative maxima, $P \approx 6.256 MPa$ and $P \approx 5.283 MPa$. The bifurcation points for the inviscid and viscous models are listed in Table 1 along with approximations for Feigenbaum's constant, δ_∞ :

$$\delta_\infty = \lim_{n \rightarrow \infty} \delta_n = \lim_{n \rightarrow \infty} \frac{E_n - E_{n-1}}{E_{n+1} - E_n}. \quad (19)$$

Feigenbaum predicted $\delta_\infty \approx 4.669201$. Both viscous and inviscid models predict δ_∞ well.

Table 1. Numerically determined bifurcation points for inviscid and viscous detonation, and approximations to Feigenbaum’s constant

	Inviscid	Inviscid	Viscous	Viscous
n	E_n	δ_n	E_n	δ_n
0	25.2650	-	27.1404	-
1	27.1875	3.86	29.3116	3.793
2	27.6850	4.26	29.8840	4.639
3	27.8017	4.66	30.0074	4.657
4	27.82675	-	30.0339	-

C. Effect of diffusion in the chaotic regime

A bifurcation diagram was constructed by sampling over 400 points with $E \in [25, 32]$, with the minimum spacing $\Delta E \approx 0.001$ occurring around $E \approx E_4$ and a maximum spacing of $\Delta E \approx 0.1$ in the stable region. For $E > E_3$, the solutions were integrated to $t = 10 \mu s$, and relative maxima in P were recorded for $t > 7 \mu s$. For $E < E_3$, solutions were only integrated to $2.5 \mu s$, and relative maxima were recorded for $t > 1 \mu s$. The late time behavior of relative maxima in P versus E is shown in Fig. 5(b), which shows the period-doubling bifurcations up to $E_\infty \approx 30.0411$. Also of note are the regions in which a limit cycle exists with an odd number of periods. For example at $E \approx 30.4$, a period-3 window exists; as E increases further, the period-3 behavior bifurcates to a period-6 behavior. It is likely that in the dense portions of the bifurcation diagram that the system is in the chaotic regime.

Figure 4 gives several plots of P versus t as E is increased. Within the chaotic regime, there exist pockets of order. Periods of 5, 6, and 3 are found and are shown in Fig. 4(c), (e), and (f), respectively. It is seen from Fig. 5 that the whole bifurcation diagram obtained by Henrick *et al.*, using a shock-fitting algorithm in which the artificial viscosity is negligibly small, occurs below the first period-doubling bifurcation of the diffusive case. Henrick *et al.* state that for $E \gtrsim 30$, the secondary captured shocks may overtake the lead shock, which would negate the accuracy of their shock-fitting technique. In the diffusive case, the system is still in the period-doubling phase at $E \approx 30$. Moreover, there is no true discontinuity; thus, the shock speed cannot be predicted as in the inviscid limit. Table 2 summarizes some the types of long time behavior realized for various values of E of viscous detonation with $L_\mu/L_{1/2} = 1/10$. Note that the table is necessarily incomplete due to the finite number of values of E sampled.

D. Effect of diminishing diffusion

By increasing the reaction length scale, $L_{1/2}$, the relative effect of diffusion decreases. Figure 6 shows solutions for $E = 27.6339$, for the ratios $L_\mu/L_{1/2}$ of (a) 1/5, (b) 1/10, and (c) 1/50. The system undergoes transition from a stable detonation to a period-1 limit cycle, to a period-2 limit cycle. The figure shows an amplitude increase in the pulsations with (a) relaxing to a $P \approx 4.213 MPa$, (b) having a relative maximum of $P_{max} \approx 4.799 MPa$ and (c) having relative maxima of $P_{max} \approx 5.578 MPa$ and $P_{max} \approx 5.895 MPa$. In addition, the frequency of the pulsations also decreases with decreasing diffusion. In the $L_\mu/L_{1/2} = 1/50$ case the period-2 behavior of the inviscid case has been recovered.

V. Conclusion

Investigation of the one-step kinetic model of one-dimensional unsteady detonation with mass, momentum, and energy diffusion has shown that the dynamics are significantly influenced in the region of instability or near instability relative to its inviscid counterpart. As in the inviscid limit, bifurcation and transition to chaos is predicted and shows similarities to the logistic map. For physically motivated reaction and diffusion length scales not unlike those for H_2 -air detonations, the addition of diffusion delays the onset of instability. As physical diffusion is reduced, the behavior of the system trends towards the inviscid limit. If the dynamics of unstable and marginally stable denotations are to be captured, physical diffusion needs to be included and needs to dominate numerical diffusion. It is likely that these results will extend to detailed kinetic systems and that detonation cell pattern formation will be influenced by the magnitude of the physical diffusion.⁹

Table 2. Ranges of different periods for viscous detonation, $L_\mu/L_{1/2} = 1/10$.

E	Period
< 27.1404	stable
[27.1404, 29.3116]	1
[29.3116, 29.8840]	2
[29.8840, 30.0074]	4
[30.0074, 30.0339]	8
[30.0600, 30.2591]	chaotic
[30.2591, 30.2788]	5
[30.2788, 30.3578]	chaotic
[30.3578, 30.3775]	5
[30.3775, 30.4071]	chaotic
[30.4071, 30.4565]	3
[30.4565, 30.4959]	6
[30.4959, 30.8512]	chaotic
[30.8512, 30.8611]	3
[30.8611, 30.9203]	6
> 30.9203	chaotic

VI. Acknowledgments

Two of the authors (CMR and JMP) recognize the support of the National Aeronautics and Space Administration (NASA) under Grant No. NNX07AD10A and the National Science Foundation (NSF) under Grant No. CBET-0650843. TDA was supported by the US Department of Energy.

References

- ¹Fedkiw, R. P., Merriman, B., and Osher, S., “High Accuracy Numerical Methods for Thermally Perfect Gas Flows with Chemistry,” *Journal of Computational Physics*, Vol. 132, No. 2, 1997, pp. 175–190.
- ²Oran, E. S., Weber, J. W., Stefaniw, E. I., Lefebvre, M. H., and Anderson, J. D., “A Numerical Study of a Two-Dimensional $H_2 - O_2 - Ar$ Detonation Using a Detailed Chemical Reaction Model,” *Combustion and Flame*, Vol. 113, No. 1-2, 1998, pp. 147–163.
- ³Hu, X. Y., Khoo, B. C., Zhang, D. L., and Jiang, Z. L., “The Cellular Structure of a Two-Dimensional $H_2/O_2/Ar$ Detonation Wave,” *Combustion Theory and Modeling*, Vol. 8, No. 2, 2004, pp. 339–359.
- ⁴Wang, B., He, H., and Yu, S. T. J., “Direct Calculation of Wave Implosion for Detonation Initiation,” *AIAA Journal*, Vol. 43, No. 10, 2005, pp. 2157–2169.
- ⁵Walter, M. A. T. and da Silva, L. F. F., “Numerical Study of Detonation Stabilization by Finite Length Wedges,” *AIAA Journal*, Vol. 44, No. 2, 2006, pp. 353–361.
- ⁶He, X. and Karagozian, A. R., “Pulse-Detonation-Engine Simulations with Alternative Geometries and Reaction Kinetics,” *Journal of Propulsion and Power*, Vol. 22, No. 4, 2006, pp. 852–861.
- ⁷Aslam, T. D. and Powers, J. M., “The Dynamics of Unsteady Detonation in Ozone,” 2009, AIAA 2009-0632.
- ⁸Tsuboi, N., Eto, K., and Hayashi, A. K., “Detailed Structure of Spinning Detonation in a Circular Tube,” *Combustion and Flame*, Vol. 149, No. 1-2, 2007, pp. 144–161.
- ⁹Powers, J. M., “Review of Multiscale Modeling of Detonation,” *Journal of Propulsion and Power*, Vol. 22, No. 6, 2006, pp. 1217–1229.
- ¹⁰Powers, J. M. and Paolucci, S., “Accurate Spatial Resolution Estimates for Reactive Supersonic Flow with Detailed Chemistry,” *AIAA Journal*, Vol. 43, No. 5, 2005, pp. 1088–1099.
- ¹¹Al-Khateeb, A. N., Powers, J. M., and Paolucci, S., “On the Necessary Grid Resolution for Verified Calculation of Premixed Laminar Flames,” *Communications in Computational Physics*, Vol. 8, No. 2, 2010, pp. 304–326.
- ¹²Erpenbeck, J. J., “Stability of Steady-State Equilibrium Detonations,” *Physics of Fluids*, Vol. 5, No. 5, 1962, pp. 604–614.
- ¹³Lee, H. I. and Stewart, D. S., “Calculation of Linear Detonation Instability: One-dimensional Instability of Planar Detonations,” *Journal of Fluid Mechanics*, Vol. 216, 1990, pp. 103–132.
- ¹⁴Bourlioux, A., Majda, A. J., and Roytburd, V., “Theoretical and Numerical Structure for Unstable One-Dimensional Detonations,” *SIAM Journal on Applied Mathematics*, Vol. 51, No. 2, 1991, pp. 303–343.

- ¹⁵Sharpe, G. J., "Linear Stability of Idealized Detonations," *Proceedings of the Royal Society of London Series A Mathematical Physical and Engineering Sciences*, Vol. 453, No. 1967, 1997, pp. 2603–2625.
- ¹⁶Kasimov, A. R. and Stewart, D. S., "On the Dynamics of Self-Sustained One-Dimensional Detonations: A Numerical Study in the Shock-Attached Frame," *Physics of Fluids*, Vol. 16, No. 10, 2004, pp. 3566–3578.
- ¹⁷Ng, H. D., Higgins, A. J., Kiyanda, C. B., Radulescu, M. I., Lee, J. H. S., Bates, K. R., and Nikiforakis, N., "Nonlinear Dynamics and Chaos Analysis of One-Dimensional Pulsating Detonations," *Combustion Theory and Modeling*, Vol. 9, No. 1, 2005, pp. 159–170.
- ¹⁸Henrick, A. K., Aslam, T. D., and Powers, J. M., "Simulations of Pulsating One-Dimensional Detonations with True Fifth Order Accuracy," *Journal of Computational Physics*, Vol. 213, No. 1, 2006, pp. 311–329.
- ¹⁹Watt, S. D. and Sharpe, G. J., "Linear and Nonlinear Dynamics of Cylindrically and Spherically Expanding Detonation Waves," *Journal of Fluid Mechanics*, Vol. 522, 2005, pp. 329–356.
- ²⁰Feigenbaum, M. J., "Quantitative Universality for a Class of Non-linear Transformations," *Journal of Statistical Physics*, Vol. 19, No. 1, 1978, pp. 25–52.
- ²¹Feigenbaum, M. J., "The Universal Metric Properties of Nonlinear Transformations," *Journal of Statistical Physics*, Vol. 21, No. 6, 1978, pp. 669–706.
- ²²Xu, S., Aslam, T. A., and Stewart, D. S., "High Resolution Numerical Simulation of Ideal and Non-ideal Compressible Reacting Flows with Embedded Internal Boundaries," *Combustion Theory and Modeling*, Vol. 1, 1997, pp. 113–142.
- ²³Oberkampf, W. L. and Trucano, T. G., "Verification and Validation in Computational Fluid Dynamics," *Progress in Aerospace Sciences*, Vol. 38, 2002, pp. 209–272.
- ²⁴Roache, P. J., "Code Verification by the Method of Manufactured Solutions," *Journal of Fluids Engineering*, Vol. 124, No. 1, 2002, pp. 4–10.
- ²⁵May, R. M., "Simple Mathematical Models with Very Complicated Dynamics," *Nature*, Vol. 261, 1976, pp. 459–467.
- ²⁶Drazin, P. G., *Nonlinear Systems*, Cambridge University Press, 1992.

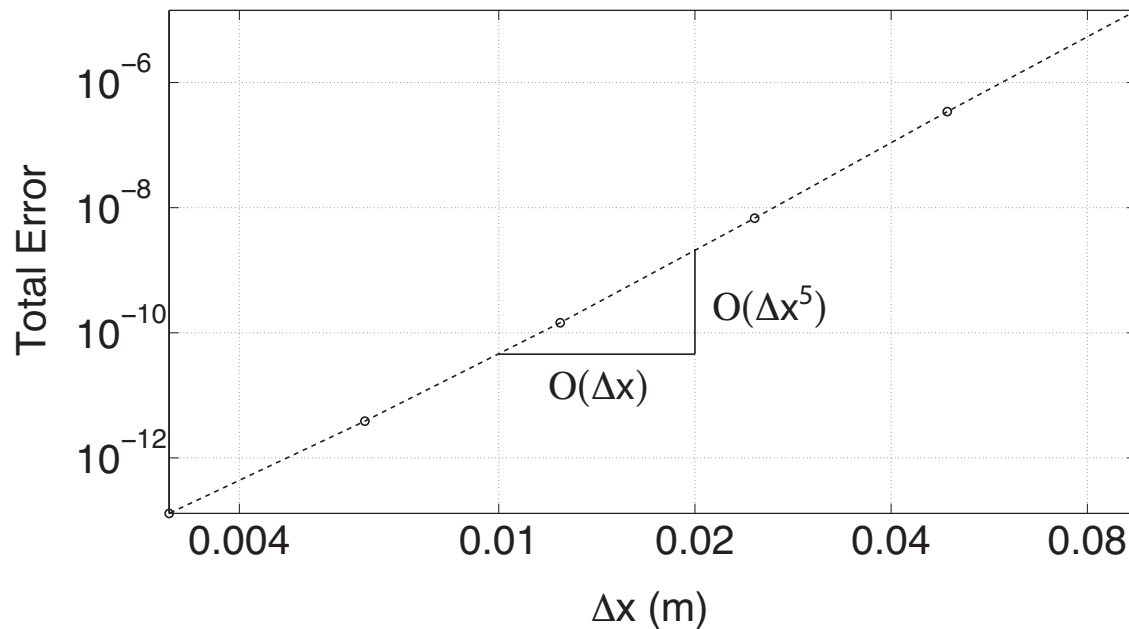


Figure 1. The normalized L_1 error versus Δx for a manufactured solution.

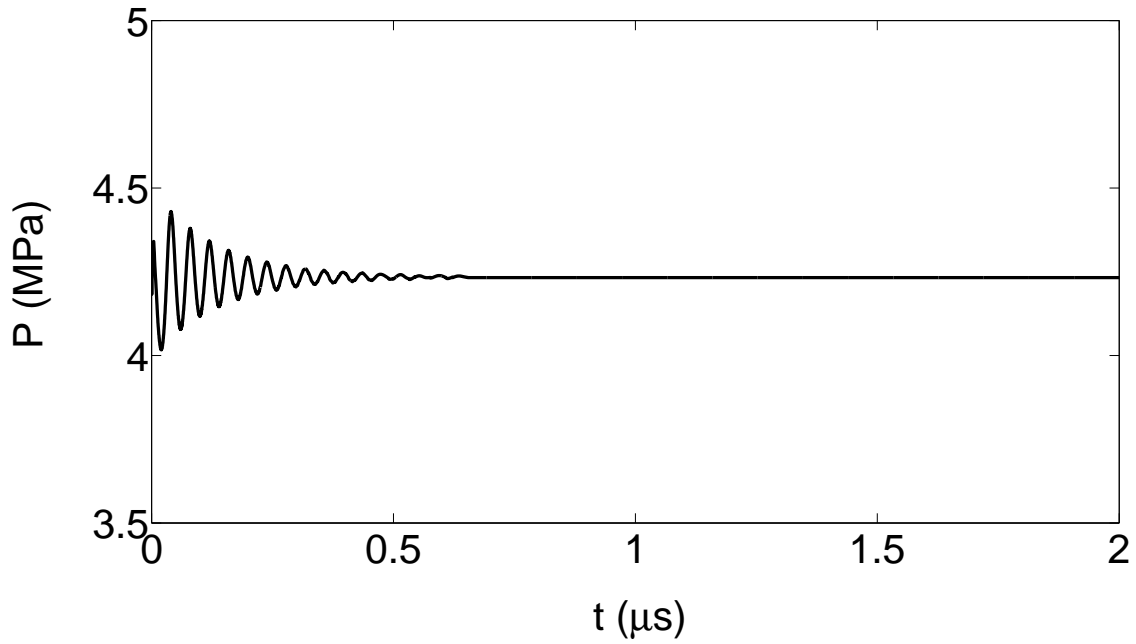


Figure 2. P versus t , $E = 26.647$, $L_\mu/L_{1/2} = 1/10$, stable viscous detonation.

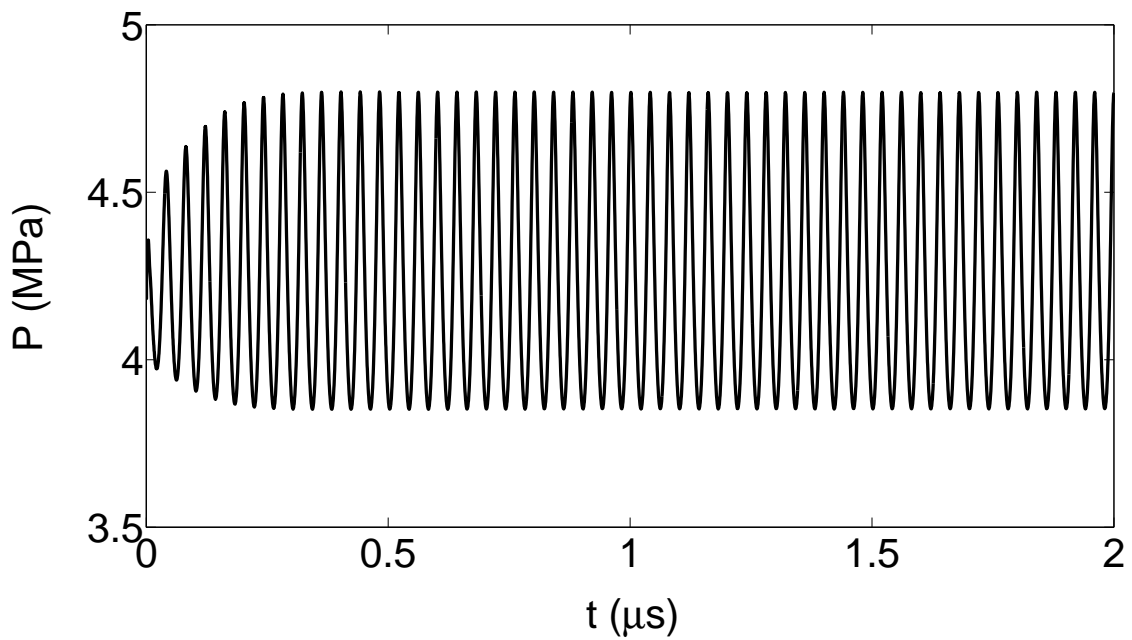


Figure 3. P versus t , $E = 27.6339$, $L_\mu/L_{1/2} = 1/10$, period-1 viscous detonation.

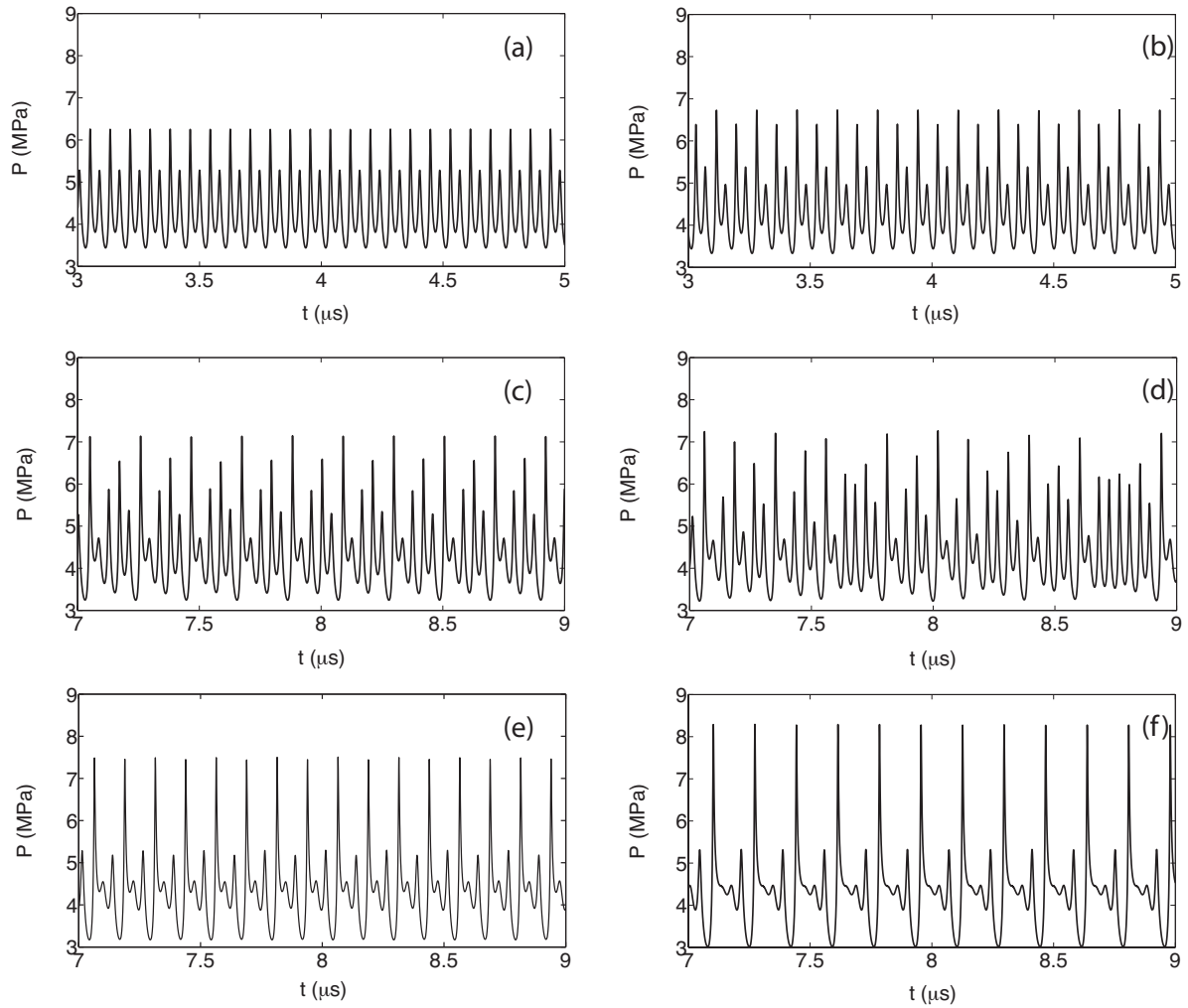
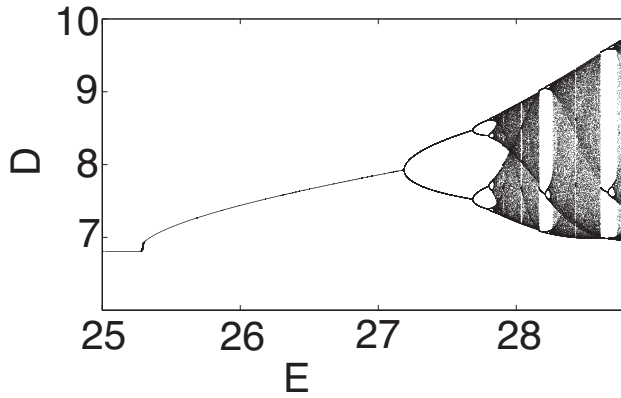
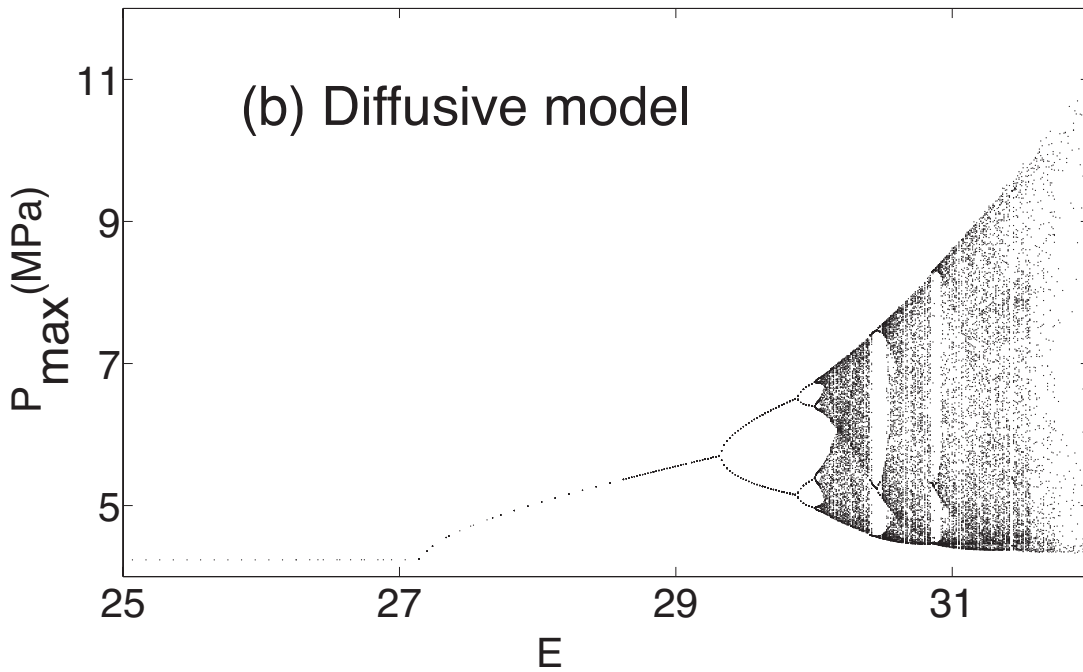


Figure 4. P versus t for viscous detonation with $L_{\mu}/L_{1/2} = 1/10$: (a) $E = 29.6077$, **period-2**, (b) $E = 30.0025$, **period-4**, (c) $E = 30.2689$, **period-5**, (d) $E = 30.3578$, **chaotic**, (e) $E = 30.4762$, **period-6**, (f) $E = 30.8512$, **period-3**.



(a) Inviscid model with shock-fitting algorithm



(b) Diffusive model

Figure 5. Comparison of numerically generated bifurcation diagrams: (a) inviscid detonation from Henrick *et al.*, (b) viscous detonation with $L_\mu/L_{1/2} = 1/10$.

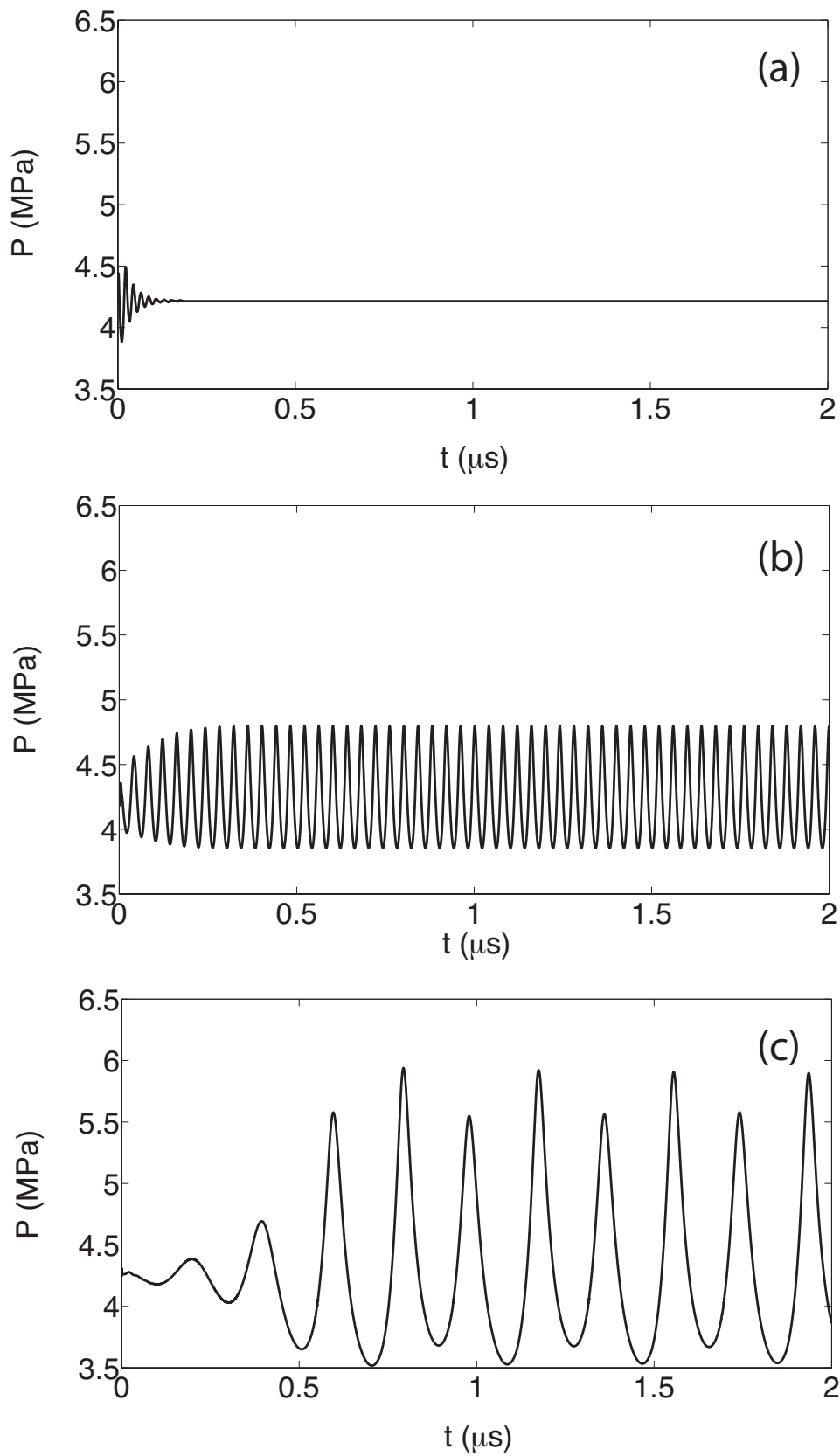


Figure 6. P versus t for viscous detonation with $E = 27.6339$ and diminishing diffusion effects: (a) $L_\mu/L_{1/2} = 1/5$, stable, (b) $L_\mu/L_{1/2} = 1/10$, period-1, (c) $L_\mu/L_{1/2} = 1/50$, period-2.